JACS
JOURNAL OF THE AMERICAN CHEMICAL SOCIETY
pubs.acs.org/JACS
Article

Controlling Ligand Coordination Spheres and Cluster Fusion in Superatoms

Douglas A. Reed, Taylor J. Hochuli, Natalia A. Gadjieva, Shoushou He, Ren A. Wiscons, Amymarie K. Bartholomew, Anouck M. Champsaur, Michael L. Steigerwald,* Xavier Roy,* and Colin Nuckolls*

Cite This: *J. Am. Chem. Soc.* 2022, 144, 306−313

ABSTRACT: We show that reaction pathways from a single superatom motif can be controlled through subtle electronic modification of the outer ligand spheres. Chevrel-type $[Co_6Se_8L_6]$ (L = PR_3, CO) superatoms are used to form carbene-terminated clusters, the reactivity of which can be influenced through the electronic effects of the surrounding ligands. This carbene provides new routes for ligand substitution chemistry, which is used to selectively install cyanide or pyridine ligands which were previously inaccessible in these cobalt-based clusters. The surrounding ligands also impact the ability of this carbene to create larger fused clusters of the type $[Co_{12}Se_{16}L_{10}]$, providing underlying information for cluster fusion mechanisms. We use this information to develop methods of creating dimeric clusters with functionalized surface ligands with site specificity, putting new ligands in specific positions on this anisotropic core. Finally, adjusting the carbene intermediates can also be used to perturb the geometry of the $[Co_6Se_8]$ core itself, as we demonstrate with a multicarbene adduct that displays a substantially anisotropic core. These additional levels of synthetic control could prove instrumental for using superatomic clusters for many applications including catalysis, electronic devices, and creating novel extended structures.

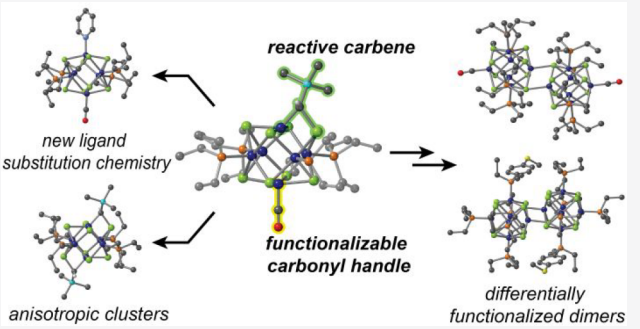

INTRODUCTION

This paper describes the ligand substitution chemistry of cobalt selenide superatomic clusters featuring a carbene motif, giving access to new surface ligands and core shapes to expand the properties of these superatoms. Many metal chalcogenide clusters are characterized by their superatom-like properties where they act as atomically precise units and feature tunable electronic structures that can be perturbed by precise modification of the exterior surface or inner core.[1−4] Because of their stability and their redox activity, these units have led to many breakthroughs in catalysis, reactivity, and electronic devices.[5−10] They have also been used as electronically, optically, or magnetically active building blocks to create extended, precise structures with emergent properties.[11−18] All of these applications require control of the outer ligand sphere as well as the shape or composition of the cluster core. To further increase the applicability of these clusters, new methods of ligand exchange, new ways of controlling ligand exchange, and procedures to synthesize new cores need to be developed.

One method to control synthetic pathways is using remote substituents on clusters with heterogeneous surface ligand sets, leveraging the tunability of specifically placed ligands to control the binding properties of other coordination sites. While this strategy is ubiquitous in standard monometallic chemistry, where variable ligand sets are used to control reaction pathways, it is difficult to accomplish within multimetallic clusters. The impacts of distant steric effects have been investigated,[6,19] but electronic effects could also be used to modulate these features. Precisely placing ligands with different electronic characteristics could be used to control ligand substitution, reactivity, or the formation of higher nuclearity cores.

Out of the many superatomic metal−chalcogenide clusters, Chevrel-type $[M_6E_8L_6]$ clusters are widely studied due to their stability and modularity with many different metals or chalcogens.[1,4,20−24] In particular, the variant $[Co_6Se_8L_6]$ (L = PR_3, CO) can be synthesized with carbon monoxide ligands placed in specific positions on the surface of the cluster to create functionalized species such as $[Co_6Se_8(CO)(PEt_3)_5]$ (**1**), $[trans\text{-}Co_6Se_8(CO)_2(PEt_3)_4]$ (**2**), and $[cis\text{-}Co_6Se_8(CO)_2(PEt_3)_4]$ (**3**).[25] These carbon monoxide ligands

Received: September 17, 2021
Published: December 23, 2021

https://doi.org/10.1021/jacs.1c09901
J. Am. Chem. Soc. 2022, 144, 306−313

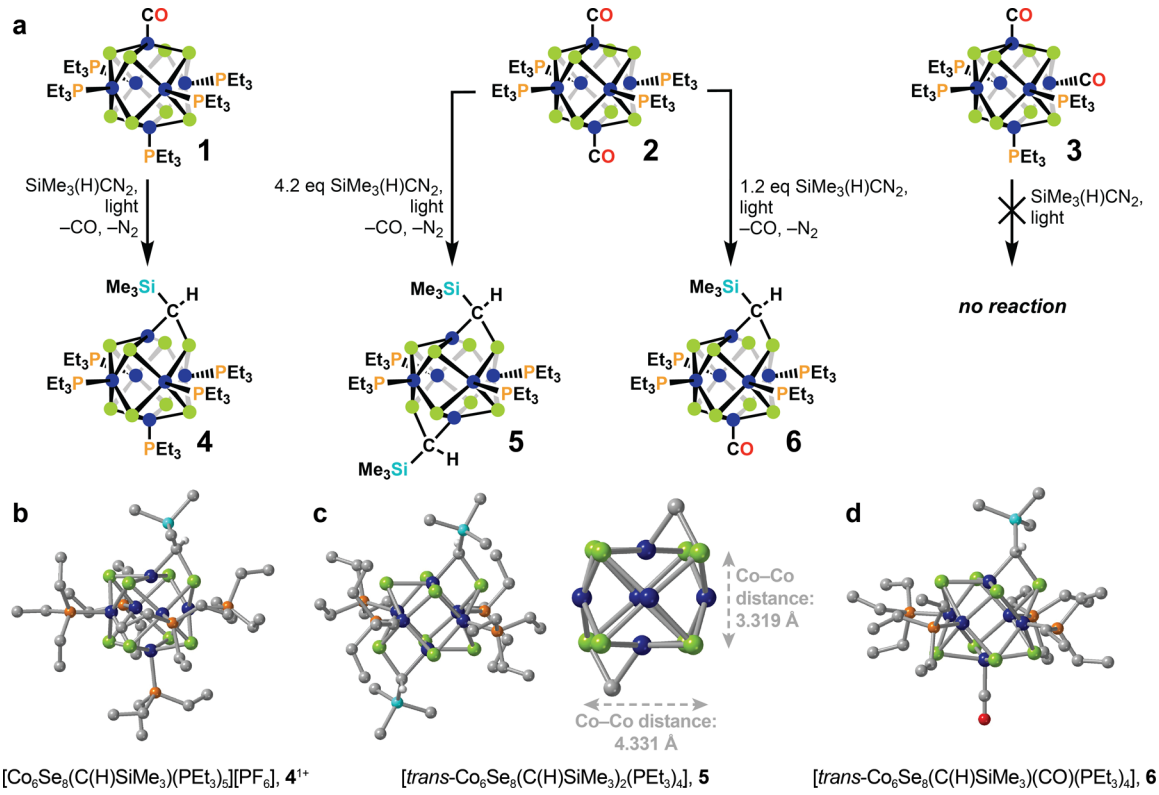

Figure 1. (a) Synthetic routes for various carbene-containing $[Co_6Se_8]$-based clusters. (b, c) Structures as determined by analysis of single-crystal X-ray diffraction are shown for (b) $[Co_6Se_8(C(H)SiMe_3)(PEt_3)_5]^{1+}$ ($\mathbf{4}^{1+}$, from ref 26) and (c) [*trans*-$Co_6Se_8(C(H)SiMe_3)_2(PEt_3)_4$] (**5**), with the anisotropic $Co_6Se_8C_2$ core of **5** highlighted. (d) The computationally predicted structure is shown for [*trans*-$Co_6Se_8(C(H)SiMe_3)(CO)(PEt_3)_4$] (**6**). Gray, white, dark blue, red, orange, green, and teal spheres correspond to C, H, Co, O, P, Se, and Si atoms, respectively. Selected H atoms, solvent molecules, counterions, and disorder are omitted to clarify the view; ellipsoid figure of **5** is shown in Figure S1.

are photolabile, allowing for facile ligand substitution chemistry at these specific positions. Furthermore, the core of this cluster can be modified directly to change the electronic or optical properties, either through metal−chalcogen bond insertion,[26] attachment of different metals to the core via surface ligands to make $[M_3Co_6Se_8]$ units (M = Fe, Co, Sn),[17,27,28] or even direct cluster fusion to make $[Co_{12}Se_{16}]$ cores.[26] Despite these advantages, designing new methods to alter these clusters could improve their function in various applications. While many diverse ligand sets have been explored, in all examples the ligands directly bound to the cobalt centers are phosphines, carbonyls, isocyanides, or carbenes,[25,26,29] ligands not traditionally used for conductive or magnetic applications. Additionally, larger clusters in the form of $[Co_{12}Se_{16}L_{10}]$,[26] where two monomeric units are directly fused through Co−Se bonds, currently have limited means of controlling site-specific functionalization of the surface ligands.

Here we show how control of the surface ligand sphere in carbene-substituted clusters $[Co_6Se_8L_6]$ (L = PEt_3, CO, $C(H)SiMe_3$) can be used to impact the ligand substitution ability, cluster fusion reactivity, or the shape of the cluster core. Through this, we can create stable cyanide and pyridine adducts previously unobserved in these clusters that may be useful for incorporation of these clusters in extended solids. Additionally, the use of different ligand sets untangles factors that influence cluster fusion to form dimeric $[Co_{12}Se_{16}L_{10}]$ clusters. Through this, methods to make site-specific functionalized dimers, where ligands are placed selectively on distinct positions on the surface, are obtained. Furthermore, we show that installing two carbenes on opposite sides of the cluster distorts the core and rearranges bonding patterns while keeping the nuclearity constant, demonstrating alternative ways of synthesizing anisotropic clusters.

RESULTS AND DISCUSSION

Synthesis of Functionalized Carbene and Multi-carbene Clusters. To understand how different ligand arrangements can impact the reactivity or structure of species containing a $:C(H)SiMe_3$ carbene, we first synthesized a series of carbene-containing clusters with different outer ligand sets. Previous studies have demonstrated that the carbonyl ligand in the monocarbonylated **1** in a reaction involving $SiMe_3(H)CN_2$ under blue light irradiation can form the carbene species $[Co_6Se_8(C(H)SiMe_3)(PEt_3)_5]$ (**4**, Figure 1a).[26] Therefore, clusters with multiple carbonyl groups such as **2** or **3** served as ideal building blocks.[25] The additional carbonyl group gives different electronic character to the overall ligand set, provides another chemical handle for further modification, or could even be used to install an additional carbene unit. However, stabilizing this carbene species on different clusters must take into account the structural changes that accompany this carbene formation. The crystal structure of the previously characterized carbene cluster shows a distorted octahedral cluster where the carbon atom of the carbene inserts itself into a cluster metal−chalcogen bond to make a Co−C−Se binding motif with a substantially elongated Co···Se distance (Figure 1b).[26] Therefore, any reactivity to make a carbene would need to be able to accommodate such cluster bonding changes.

Reaction of **2** with various amounts of $SiMe_3(H)CN_2$ afforded new carbene-cluster species (Figure 1a). When we

https://doi.org/10.1021/jacs.1c09901
J. Am. Chem. Soc. 2022, 144, 306−313

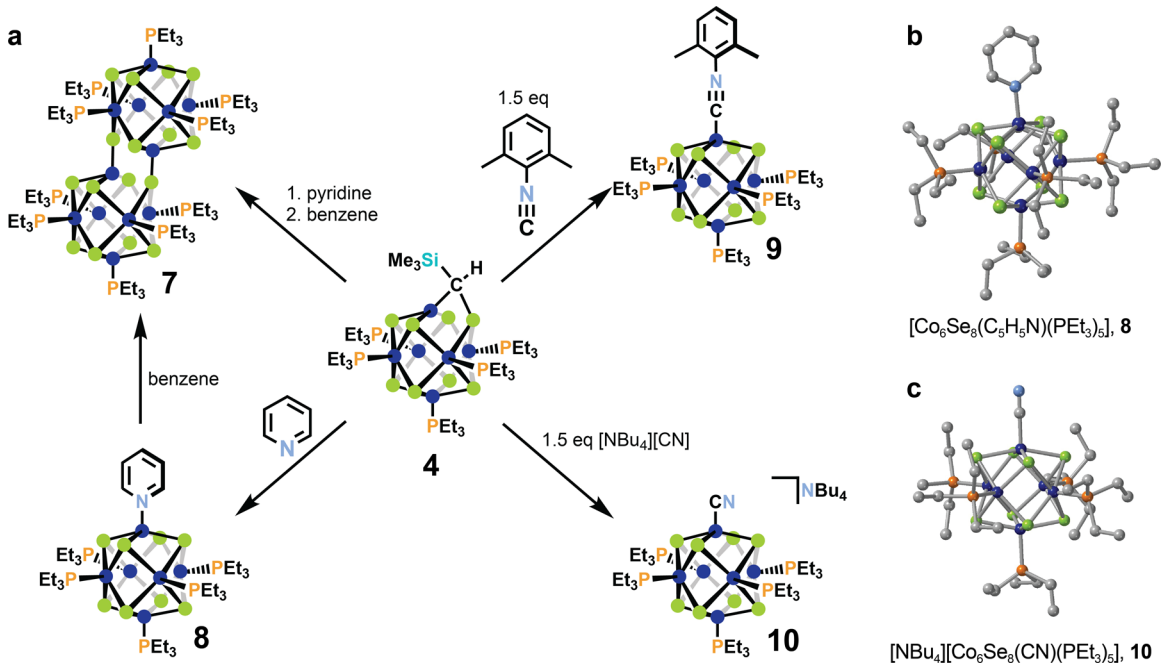

Figure 2. (a) Reaction pathways starting with $[Co_6Se_8(C(H)SiMe_3)(PEt_3)_5]$ (**4**), detailing the synthesis of $[Co_{12}Se_{16}(PEt_3)_{10}]$ (**7**), $[Co_6Se_8(C_5H_5N)(PEt_3)_5]$ (**8**), $[Co_6Se_8(CNC_6H_3Me_2)(PEt_3)_5]$ (**9**), and $[NBu_4][Co_6Se_8(CN)(PEt_3)_5]$ (**10**). (b, c) Structures as determined by analysis of single-crystal X-ray diffraction are shown for (b) **8** and (c) **10**. Gray, dark blue, light blue, orange, and green spheres correspond to C, Co, N, P, and Se atoms, respectively. H atoms, solvent molecules, counterions, and disorder are omitted to clarify the view; ellipsoid figures of **8** and **10** are shown in Figures S2 (**8**) and S3 (**10**).

add a large molar excess (4.2 equiv) and irradiate under blue light, infrared spectroscopy shows the complete disappearance of CO after 3 h (Figure S6). Single-crystal X-ray diffraction data gave the structure $[trans\text{-}Co_6Se_8(C(H)SiMe_3)_2(PEt_3)_4]$ (**5**), which now has two antipodal carbene species with elongated Co···Se distances (Figure 1c) to result in an anisotropic cluster where the sides containing the carbene-inserted bonds are much longer than the remaining sides. Through-cluster Co···Co distances show a very large distortion, registering 4.331 Å on the long axis and over an angstrom shorter at 3.319 Å in the shortest direction (Figure 1c) versus the 4.153 Å in all directions in the homogeneously substituted $[Co_6Se_8(PEt_3)_6]$.[30] This is a substantial deviation from standard coordination chemistry on these clusters, as the cluster geometries and these metal−metal distances are generally unchanged by standard ligand substitution reactions even with very electronically different species.[31] While anisotropic cores with different nuclearities are known,[32−35] this demonstrates that high degrees of distortion are attainable starting with an otherwise isotropic core. Expanding the diversity of these clusters could be further optimized through this different method of distorting these clusters.

When instead we treat **2** with less $SiMe_3(H)CN_2$ (1.2 equiv, Figure 1a), a different species emerges. Unlike in the case above, in this instance infrared spectroscopy shows this new species retains a carbonyl group (Figure S7). We assign this new product as the monosubstituted carbene species $[trans\text{-}Co_6Se_8(C(H)SiMe_3)(CO)(PEt_3)_4]$ (**6**). While we were not able to isolate single crystals suitable for diffraction, we have produced calculated structures (determined via DFT using B3LYP-D3 functional and 6-31g**/LACVP** basis sets; see the Supporting Information) that indicate that a similar motif of an inserted carbon atom within the Co···Se interaction is observed (Figure 1d). The presence of a carbon monoxide group gives a direct handle for further functionalization and also can be used to modify the reactivity of the carbene.

Interestingly, changing the regiochemistry of the starting carbonylated cluster changes the reactivity dramatically. Despite the ability of **2** to form carbene-containing species with $SiMe_3(H)CN_2$, under similar conditions carbene formation does not occur starting with **3**, where the only difference is the relative position of these carbonyl species (Figure 1a). Instead, quantitative recovery of the starting cluster and various diazo decomposition products are observed. To our knowledge, this divergent reactivity between **2** and **3** is the first example where these isomers behave differently, as in standard ligand substitution reactions these species behave identically.[25] While nominally the electron density is distributed evenly among all cobalt centers, previous studies have demonstrated that the carbonyl-ligated cobalt centers show are more electron-deficient relative to phosphine-ligated cobalt centers.[31] The different ligand arrangements and clustering of these electron-deficient centers could explain this difference in diazoalkane activation and could be used in the future to influence reactivity pathways in superatoms. In this case, we use this to show that the electronic influences of distant sites can be used to deactivate ligand substitution patterns in these clusters.

Reactivity of $[Co_6Se_8(C(H)SiMe_3)(PEt_3)_5]$ (4). The distorted Co−C−Se bond and the relatively accessible cobalt center in the carbene-containing **4** indicated that ligand substitution might be possible at this position. Initial work on the reactivity of **4** focused exclusively on a cluster fusion reaction to form the dimeric, fused cluster, $[Co_{12}Se_{16}(PEt_3)_{10}]$ (**7**), where the carbene ligands on two separate clusters are replaced by direct Co−Se bonds between the two monomeric units (Figure 2a).[26] In exploring this reaction, we found that this same reaction can be induced by completely dissolving the

https://doi.org/10.1021/jacs.1c09901
J. Am. Chem. Soc. 2022, 144, 306−313

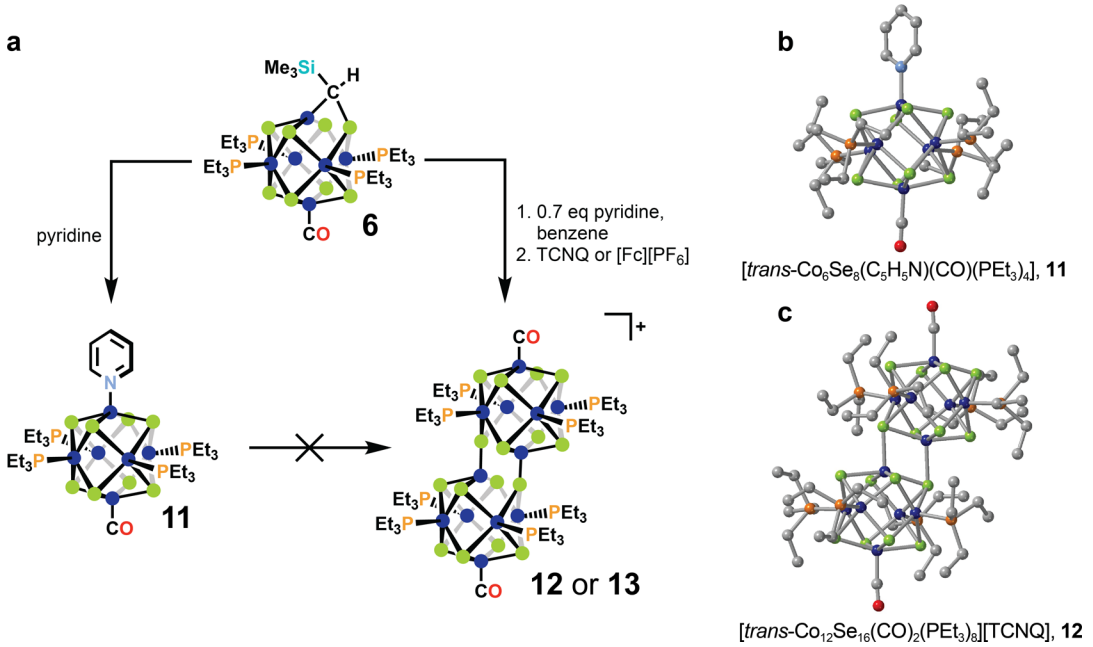

Figure 3. (a) Reaction pathways starting with [*trans*-$Co_6Se_8(C(H)SiMe_3)(CO)(PEt_3)_4$] (**6**), detailing the synthesis of [*trans*-$Co_6Se_8(C_5H_5N)(CO)(PEt_3)_4$] (**11**) and [*trans*-$Co_{12}Se_{16}(CO)_2(PEt_3)_8]^{1+}$ (**12** or **13**). (b, c) Structures as determined by analysis of single-crystal X-ray diffraction are shown for (b) **11** and (c) **12** (TCNQ = tetracyanoquinodimethane). Gray, dark blue, light blue, red, orange, and green spheres correspond to C, Co, N, O, P, and Se atoms, respectively. H atoms, solvent molecules, counterions, and disorder are omitted to clarify the view; ellipsoid figures of **11** and **12** are shown in Figure S4 (**11**) and Figure S5 (**12**).

carbene species in pyridine, removing the pyridine *in vacuo*, and then dissolving this new species in benzene to form **7** (Figure 2a), suggesting that pyridine might be participating in this reaction. After dissolution in pyridine, crystallization of the cluster directly from pyridine afforded the pyridine-substituted $[Co_6Se_8(C_5H_5N)(PEt_3)_5]$ (**8**) where the pyridine has completely replaced the carbene ligand (Figure 2b).

This result shows that direct substitution of the carbene with other ligands is possible utilizing mild reaction conditions and gives an alternate route for ligand substitution than previously accessible in these clusters. While pyridine coordination has been observed for similar clusters containing different transition metals,[18,36] to our knowledge this pyridine termination has not been observed for any $[Co_6E_8]$ cluster. Notably, attempting pyridine ligand exchange by directly replacing the carbonyl group in **1** through standard photo-induced carbonyl substitution was not successful. As a simple proof that this method of ligand substitution is generalizable, we used the carbene cluster as a starting material for previously studied isocyanide-ligated clusters.[25] Addition of 2,6-dimethylphenyl isocyanide to **4** at room temperature generates $[Co_6Se_8(CNC_6H_3Me_2)(PEt_3)_5]$ (**9**, Figure 2a). This compound has previously been prepared by irradiating a solution of **1** and 2,6-dimethylphenyl isocyanide and with blue light;[25] the reaction of the carbene avoids the intense irradiation.

Using these new reaction conditions, we can now access coordinating ligands that are not obtainable through photolytic substitution of CO. We demonstrate this by installing a single cyanide group to form $[NBu_4][Co_6Se_8(CN)(PEt_3)_5]$ (**10**, Figure 2a). A cyano group, commonly used in the formation of extended structures with interesting magnetic and electronic properties,[37,38] has been utilized as a ligand in other M_6E_8 clusters to make cluster-based materials.[14,39] However, this ligand has not been installed on superatomic clusters with site specificity, which would allow for more controlled synthesis of extended solids. While the $[Co_6Se_8]$ cores with carbonyl groups stand as ideal platforms, replacing the CO group of **1** with CN^- cannot be induced by using standard thermal or photolytic conditions. Addition of tetrabutylammonium cyanide in toluene to **4** yields **10**. Various characterization methods are used to show the distinction from the similar **1**. Analysis of single-crystal X-ray diffraction data (Figure 2c) shows that the bond length found for $Co-C_{CN}$ (1.846 Å) is longer than that of the $Co-C_{CO}$ bond (1.737 Å) found in **1**,[25] and infrared spectroscopy shows a clear, single ν_{CN} stretch of 2093 cm^{-1} (Figure S9). Cyclic voltammetry measurements (Figure S13) demonstrate that the cluster displays reversible redox activity with two waves at −1.15 and −0.4 V, which we assign to the $[Co_6Se_8(CN)(PEt_3)_5]^{2-/1-}$ and $[Co_6Se_8(CN)(PEt_3)_5]^{1-/0}$ redox couples. Importantly, this is the first example of the $[Co_6Se_8L_6]^{1-}$ core (the reduced form of **10**) being isolated in these specific types of clusters; in the standard phosphine-, carbonyl-, or isocyanide-ligated species, the reduction events past neutral are asymmetric, sometimes irreversible, and occur at very negative potentials.[26] We do note that this ligand exchange requires an excess (1.5 equiv) of the substituting ligand. When using a substoichiometric amount of cyanide, decomposition products are visible as assessed by infrared spectroscopy (Figure S10). This gives some indication that this approach for ligand substitution may require some optimization for each specific ligand.

Reactivity of [*trans*-$Co_6Se_8(C(H)SiMe_3)(CO)(PEt_3)_4$] (6). We then investigated the reactivity or cluster fusion ability of the carbene-containing **6** to probe the impact of the electron-withdrawing carbonyl group. Dissolution of **6** in pyridine resulted in the replacement of the carbene ligand with pyridine to form [*trans*-$Co_6Se_8(C_5H_5N)(CO)(PEt_3)_4$] (**11**, Figures 3a and 3b). This demonstrates that both carbene species **6** and **4** react similarly. However, the two resultant pyridine-ligated clusters, **8** and **11**, show very different properties. A dramatic

https://doi.org/10.1021/jacs.1c09901
J. Am. Chem. Soc. 2022, 144, 306−313

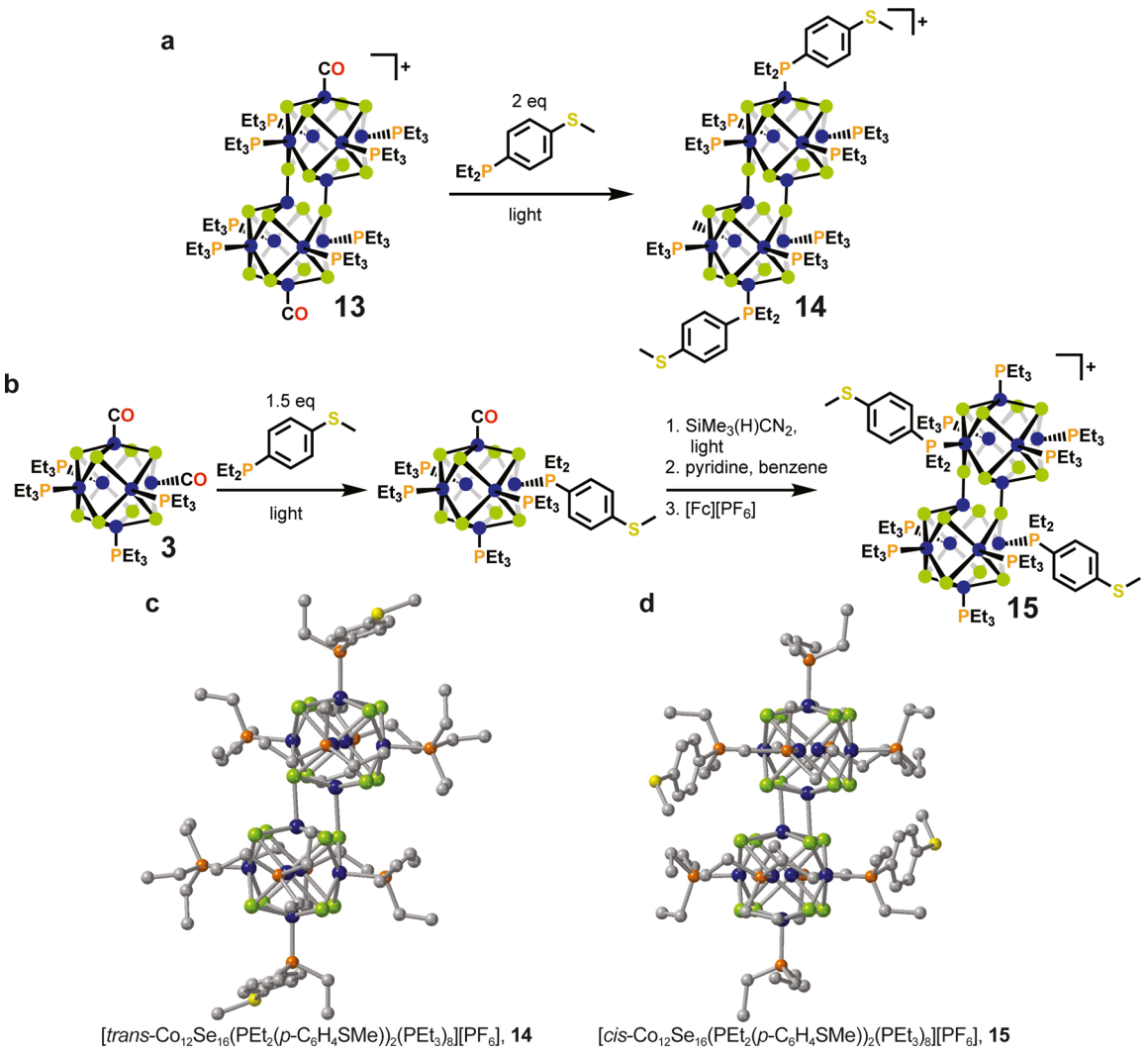

Figure 4. (a, b) Synthesis of functionalized $[Co_{12}Se_{16}L_{10}]$ dimers through two different methods. (a) Method of direct ligand substitution of [*trans*-$Co_{12}Se_{16}(CO)_2(PEt_3)_8$][$PF_6$] (**13**) through photolysis of CO ligands, highlighting the synthesis of [*trans*-$Co_{12}Se_{16}(PEt_2(p\text{-}C_6H_4SMe))_2(PEt_3)_8$]-[$PF_6$] (**14**). (b) Method of fusion of substituted $[Co_6Se_8(CO)_2(PEt_3)_4]$ isomers, highlighting the synthesis of [*cis*-$Co_{12}Se_{16}(PEt_2(p\text{-}C_6H_4SMe))_2(PEt_3)_8]^{1+}$ (**15**) starting with [*cis*-$Co_6Se_8(CO)_2(PEt_3)_4$] (**3**). (c, d) Structures as determined by analysis of single-crystal X-ray diffraction are shown for (c) **14** (from ref 9) and (d) **15**. Gray, dark blue, orange, yellow, and green spheres correspond to C, Co, P, S, and Se atoms, respectively. H atoms, solvent molecules, counterions, and disorder are omitted to clarify the view.

change occurs in the cluster fusion reaction, as dissolving **8** in noncoordinating solvents such as benzene rapidly forms $[Co_{12}Se_{16}]$ fused products (Figure 2a), whereas under these conditions **11** remains undisturbed (Figure 3a). Trying many variations on these conditions to induce fusion with **11**, such as applying heat, irradiating with light, or adding oxidants, as have been used in previous examples of cluster fusion,[26,40−42] still did not result in dimer formation. This conclusively shows the dramatic differences in various cluster−ligand interactions by changing remote substituents. Additionally, by use of this specifically positioned carbonyl group, pyridine ligands are stabilized on these cobalt−chalcogenide clusters, and as such they can be used in even more applications that can take advantage of the ability of pyridine to induce magnetic coupling[43] or accept electron density in metal−ligand charge-transfer applications.[44]

While a stable pyridine adduct was interesting, dimeric species with photolabile CO ligands could still be useful in many applications. Despite the stability of the pyridine adduct **11**, excitingly the carbene in **6** can still be used to create fused dimeric species with these accessible carbonyl handles. As discussed previously in the synthesis of **10**, adding varying amounts of cyanide ions to a carbene cluster leads to different reactivity. We found that addition of a substoichiometric amount of pyridine to a solution of **6** in benzene resulted in successful fusion to create the dimeric species [*trans*-$Co_{12}Se_{16}(CO)_2(PEt_3)_8$] in a mixture with a small amount of **11** side product (Figure 3a). The more negative oxidation potential of $Co_{12}Se_{16}$ cores[9,26] allows for selective oxidation of the dimer to form [*trans*-$Co_{12}Se_{16}(CO)_2(PEt_3)_8]^{1+}$ upon addition of an oxidant. This charged species can be then cleanly separated from the remaining neutral monomeric side product. Using tetracyanoquinodimethane (TCNQ) as an oxidant, crystals of [*trans*-$Co_{12}Se_{16}(CO)_2(PEt_3)_8$][TCNQ] (**12**) suitable for X-ray diffraction were obtained (Figure 3c). As was expected given the ligand arrangements on the starting monomer, the carbonyl ligands are selectively positioned at the end of the long axis of the cluster.

Importantly, installing labile carbonyl ligands on the dimer does not impact the stability of the cluster when accessing the

https://doi.org/10.1021/jacs.1c09901
J. Am. Chem. Soc. 2022, 144, 306−313

electronic properties of the inner core. Cyclic voltammetry measurements of [*trans*-$Co_{12}Se_{16}(CO)_2(PEt_3)_8$][$PF_6$] (**13**) show many reversible redox waves, with five features between −2.0 and 0.7 V versus Fc/Fc^+ (Fc = ferrocene, Figure S14). Because of the electron-withdrawing character of the carbon monoxide ligands, the positions of these waves are slightly shifted relative to that of other [$Co_{12}Se_{16}L_{10}$] congeners completely ligated by phosphine ligands.[9,26] Interestingly, this shift (+0.3 V) is similar to that seen for the transition from [$Co_6Se_8(PEt_3)_6$] to monocarbonylated **1**,[25] which features nearly the same ratio of phosphine-to-carbonyl ligand replacement.

Synthesis of Functionalized Dimeric Species. Creating clusters with ligands in specific positions can be integral to unlocking new properties or reactivity. Therefore, we sought to make substituted dimeric [$Co_{12}Se_{16}L_{10}$] units. These dimeric species are more optically and electronically active than their monomeric counterparts[9,26] and could result in internal magnetic and electronic internal fields unique among clusters for various applications,[45,46] and the anisotropic structure induces different types of crystal packing than can be accessible with standard symmetric clusters.[47] All of these features could be tuned or enhanced by using site-specific ligand sets. Using **13**, the carbonyl groups could be photolytic handles for installing different ligands on the ends of the long axis of the cluster. Replacing the carbonyl group with the phosphine ligand $PEt_2(p\text{-}C_6H_4SMe)$ served as a reasonable case study, as the cluster [*trans*-$Co_{12}Se_{16}(PEt_2(p\text{-}C_6H_4SMe))_2(PEt_3)_8$][$PF_6$] (**14**) has been synthesized and characterized previously.[9] Reaction of **13** with $PEt_2(p\text{-}C_6H_4SMe)$ under blue light irradiation gives the species **14** (Figures 4a,c). This method can likely be extended to different ligands to create even more diverse dimeric species.

While this is a direct method toward making functionalized dimeric species with differentiated ligands at the ends of the long axis of the cluster, selectively installing new ligands at different positions requires an alternative approach. The possible *cis*-ligated building block **3** cannot be used to stabilize a carbene precursor toward the final fused dimers, as having carbonyl groups in this arrangement prevents any reactivity with carbene-generating precursors (Figure 1a). Therefore, directly making [$Co_{12}Se_{16}$] cores decorated with carbonyl groups at different position than seen in **13** cannot be accessed, and direct photolytic substitution for ligand exchange cannot be used.

Despite this limitation, we present a general strategy for making functionalized dimers by preinstalling ligands before cluster fusion (Figure 4b). Given our understanding that cluster fusion is mediated by the relative stability of pyridine-ligated intermediates, synthesizing monomers with five electron-donating ligands—such as phosphines—and one carbonyl ligand should be suitable building blocks. This unit can be converted stepwise into a carbene-ligated cluster, then a pyridine-ligated cluster, and finally fused to become a dimeric unit. The dimeric species will show a more negative oxidation potential than the remaining monomeric side products,[9,26] allowing for selective oxidation and then extraction of the desired dimeric species. Starting with **3**, replacing one of the ligands with a different ligand (R) such as a phosphine or isocyanide using photolytic substitution yields these candidates in the form of [*cis*-$Co_6Se_8R(CO)(PEt_3)_4$] as a precursor to make new *cis*-functionalized dimers. We found that the most effective conversion through this route involves adding 1.5 equiv of new ligand R to **3**. This reaction forms a 1:1 mixture of the desired intermediate [*cis*-$Co_6Se_8R(CO)(PEt_3)_4$] and the side product [*cis*-$Co_6Se_8R_2(PEt_3)_4$]. While these products are difficult to separate at this stage, this side product does not impact the rest of the cluster fusion reaction and can be separated during the selective oxidation and extraction of the desired dimeric species. We note that this strategy was previously employed by our groups to make **14** by starting with **2**,[9] demonstrating the generalizability of this strategy.

By starting with **3** and preinstalling $PEt_2(p\text{-}C_6H_4SMe)$, this procedure yielded the new species [*cis*-$Co_{12}Se_{16}(PEt_2(p\text{-}C_6H_4SMe))_2(PEt_3)_8$][$PF_6$] (**15**, Figure 4d). The differentiated $PEt_2(p\text{-}C_6H_4SMe)$ ligands are now located on the short axis of the cluster and are placed selectively on opposite sides. Interestingly, this particular arrangement is the same as that reported in a similarly functionalized [$Re_{12}Se_{16}$] core.[40] Construction using different ligands or even bridging ligands could enable greater control of the possible regiochemistry present within this modified [$Co_{12}Se_{16}$] dimer. Despite the different ligand arrangement of **15** compared to **14**, we find that the redox properties of **14** and **15** are nearly identical (Figure S15).[9] Five fully reversible redox couples between −2.0 and +0.3 V are observed, demonstrating that the electronic properties of the cluster core can be preserved while the modifying the surface ligand geometry. This is similar to previously reported regioisomeric clusters.[9,25] However, using this method to install different types of ligands could be key to unlocking new electronic properties in these [$Co_{12}Se_{16}L_{10}$] dimers. Additionally, by using even more types of carbonylated starting materials, such as [*mer*-$Co_6Se_8(CO)_3(PEt_3)_3$], [*fac*-$Co_6Se_8(CO)_3(PEt_3)_3$], or other variants observed with other phosphines,[25] we envision creating a much larger library of functionalized dimeric species with an array of different properties.

CONCLUSIONS

The ability to make new clusters with atomically precise ligand coordination spheres and cluster nuclearity is an important means to unlock new reactivity and electronic properties within the versatile metal chalcogenide systems. Using carbene or multicarbene adducts, we explored new methods of performing these transformations that circumvent traditional photolytic or thermal methods. We think these new methods could be generalizable over many types of clusters. Additionally, these synthetic modifications can be more accurately controlled by the electronic properties of remote substituents. This is demonstrated with clusters containing specifically placed surface carbonyl groups that can alter distant carbene ligand substitution or the lability of remote pyridine groups to impact cluster fusion.

These results also lay the foundation for making new cluster-containing materials, as many of these species could be key building blocks for extended coordination solids. Cyanide and pyridine ligands, first accessed in these cobalt-containing clusters here, have been demonstrated to make extended networks.[14,17,18,39] Research is currently underway to synthesize these exciting materials that can take advantage of the redox activity and paramagnetic character of these units. Additionally, making larger, atomically precise clusters beyond those shown here has been predicted to make new types of electronic properties through emergent quantum confinement effects in nanometer-sized cores.[26] Controlling further cluster fusion is currently underway starting with either **13**, the

https://doi.org/10.1021/jacs.1c09901
J. Am. Chem. Soc. 2022, 144, 306−313

carbonyl groups of which could be modified make fusion precursors, or **5**, which already serves as an ideal platform for making new cobalt−selenide nanoclusters and nanowires with highly controlled surface functionalities.

■ ASSOCIATED CONTENT

Supporting Information

The Supporting Information is available free of charge at https://pubs.acs.org/doi/10.1021/jacs.1c09901.

Full experimental details, materials, and methods, computational details, additional crystallographic data, infrared spectroscopy characterization data, and additional electrochemical characterization data (PDF)

Accession Codes

CCDC 2110276−2110280 and 2111707 contain the supplementary crystallographic data for this paper. These data can be obtained free of charge via www.ccdc.cam.ac.uk/data_request/cif, or by emailing data_request@ccdc.cam.ac.uk, or by contacting The Cambridge Crystallographic Data Centre, 12 Union Road, Cambridge CB2 1EZ, UK; fax: +44 1223 336033.

■ AUTHOR INFORMATION

Corresponding Authors

Michael L. Steigerwald − *Department of Chemistry, Columbia University, New York, New York 10027, United States*; Email: mls2064@columbia.edu

Xavier Roy − *Department of Chemistry, Columbia University, New York, New York 10027, United States*; orcid.org/0000-0002-8850-0725; Email: xr2114@columbia.edu

Colin Nuckolls − *Department of Chemistry, Columbia University, New York, New York 10027, United States*; orcid.org/0000-0002-0384-5493; Email: cn37@columbia.edu

Authors

Douglas A. Reed − *Department of Chemistry, Columbia University, New York, New York 10027, United States*; orcid.org/0000-0001-5170-9050

Taylor J. Hochuli − *Department of Chemistry, Columbia University, New York, New York 10027, United States*

Natalia A. Gadjieva − *Department of Chemistry, Columbia University, New York, New York 10027, United States*

Shoushou He − *Department of Chemistry, Columbia University, New York, New York 10027, United States*

Ren A. Wiscons − *Department of Chemistry, Columbia University, New York, New York 10027, United States*

Amymarie K. Bartholomew − *Department of Chemistry, Columbia University, New York, New York 10027, United States*

Anouck M. Champsaur − *Department of Chemistry, Columbia University, New York, New York 10027, United States*

Complete contact information is available at: https://pubs.acs.org/10.1021/jacs.1c09901

Notes

The authors declare no competing financial interest.

■ ACKNOWLEDGMENTS

Support for this research was provided by the by the Center for Precision-Assembled Quantum Materials, an NSF MRSEC (Award DMR-2011738), Air Force Office of Scientific Research (Award FA9550-18-1-0020), and the National Science Foundation under Award CBET-2017198. D.A.R. thanks the Columbia Nano Initiative for Postdoctoral Fellowship support. R.A.W. and A.K.B. thank the Arnold O. Beckman Foundation for Postdoctoral Fellowship support. Single-crystal X-ray diffraction analysis was performed at the Shared Materials Characterization Laboratory (SMCL) at Columbia University. Use of the SMCL was made possible by funding from Columbia University.

■ REFERENCES

(1) McCleverty, J. A.; Meyer, T. J. *Comprehensive Coordination Chemistry II: From Biology to Nanotechnology*, 1st ed.; Elsevier: Amsterdam, 2004.

(2) Doud, E. A.; Voevodin, A.; Hochuli, T. J.; Champsaur, A. M.; Nuckolls, C.; Roy, X. Superatoms in Materials Science. *Nat. Rev. Mater.* **2020**, *5* (5), 371−387.

(3) Fedorov, V. E.; Mishchenko, A. V.; Fedin, V. P. Cluster Transition Metal Chalcogenide Halides. *Russ. Chem. Rev.* **1985**, *54* (4), 408−423.

(4) Lin, Z.; Williams, I. D. Structure and Bonding in Face- and Edge-Bridged Octahedral Transition Metal Clusters. *Polyhedron* **1996**, *15*, 3277−3287.

(5) McAllister, J.; Bandeira, N. A. G.; McGlynn, J. C.; Ganin, A. Y.; Song, Y. F.; Bo, C.; Miras, H. N. Tuning and Mechanistic Insights of Metal Chalcogenide Molecular Catalysts for the Hydrogen-Evolution Reaction. *Nat. Commun.* **2019**, *10* (1), 370.

(6) Venkateswara Rao, P.; Holm, R. H. Synthetic Analogues of the Active Sites of Iron-Sulfur Proteins. *Chem. Rev.* **2004**, *104* (2), 527−559.

(7) Beecher, A. N.; Yang, X.; Palmer, J. H.; Lagrassa, A. L.; Juhas, P.; Billinge, S. J. L.; Owen, J. S. Atomic Structures and Gram Scale Synthesis of Three Tetrahedral Quantum Dots. *J. Am. Chem. Soc.* **2014**, *136* (30), 10645−10653.

(8) Lovat, G.; Choi, B.; Paley, D. W.; Steigerwald, M. L.; Venkataraman, L.; Roy, X. Room-Temperature Current Blockade in Atomically Defined Single-Cluster Junctions. *Nat. Nanotechnol.* **2017**, *12* (11), 1050−1054.

(9) Gunasekaran, S.; Reed, D. A.; Paley, D. W.; Bartholomew, A. K.; Venkataraman, L.; Steigerwald, M. L.; Roy, X.; Nuckolls, C. Single-Electron Currents in Designer Single-Cluster Devices. *J. Am. Chem. Soc.* **2020**, *142* (35), 14924−14932.

(10) Liu, J.; Kelley, M. S.; Wu, W.; Banerjee, A.; Douvalis, A. P.; Wu, J.; Zhang, Y.; Schatz, G. C.; Kanatzidis, M. G. Nitrogenase-Mimic Iron-Containing Chalcogels for Photochemical Reduction of Dinitrogen to Ammonia. *Proc. Natl. Acad. Sci. U. S. A.* **2016**, *113* (20), 5530−5535.

(11) Baek, W.; Bootharaju, M. S.; Walsh, K. M.; Lee, S.; Gamelin, D. R.; Hyeon, T. Highly Luminescent and Catalytically Active Superstructures of Magic-Sized Semiconductor Nanoclusters. *Nat. Mater.* **2021**, *20*, 650−657.

(12) Roy, X.; Lee, C. H.; Crowther, A. C.; Schenck, C. L.; Besara, T.; Lalancette, R. A.; Siegrist, T.; Stephens, P. W.; Brus, L. E.; Kim, P.; Steigerwald, M. L.; Nuckolls, C. Nanoscale Atoms in Solid-State Chemistry. *Science* **2013**, *341* (6142), 157−160.

(13) Xie, J.; Wang, L.; Anderson, J. S. Heavy Chalcogenide-Transition Metal Clusters as Coordination Polymer Nodes. *Chem. Sci.* **2020**, *11* (32), 8350−8372.

(14) Bennett, M. V.; Beauvais, L. G.; Shores, M. P.; Long, J. R. Expanded Prussian Blue Analogues Incorporating $[Re_6Se_8(CN)_6]^{3-/4-}$ Clusters: Adjusting Porosity via Charge Balance. *J. Am. Chem. Soc.* **2001**, *123* (33), 8022−8032.

(15) Champsaur, A. M.; Mézière, C.; Allain, M.; Paley, D. W.; Steigerwald, M. L.; Nuckolls, C.; Batail, P. Weaving Nanoscale Cloth through Electrostatic Templating. *J. Am. Chem. Soc.* **2017**, *139* (34), 11718−11721.

(16) Champsaur, A. M.; Yu, J.; Roy, X.; Paley, D. W.; Steigerwald, M. L.; Nuckolls, C.; Bejger, C. M. Two-Dimensional Nanosheets from Redox-Active Superatoms. *ACS Cent. Sci.* **2017**, *3* (9), 1050−1055.
(17) Kephart, J. A.; Romero, C. G.; Tseng, C. C.; Anderton, K. J.; Yankowitz, M.; Kaminsky, W.; Velian, A. Hierarchical Nanosheets Built from Superatomic Clusters: Properties, Exfoliation and Single-Crystal-to-Single-Crystal Intercalation. *Chem. Sci.* **2020**, *11* (39), 10744−10751.
(18) Selby, H. D.; Orto, P.; Zheng, Z. Supramolecular Arrays of the $[Re_6([\mu_3\text{-}Se)_8]^{2+}$ Core-Containing Clusters Mediated by Transition Metal Ions. *Polyhedron* **2003**, *22* (22), 2999−3008.
(19) Brown, A. C.; Suess, D. L. M. Controlling Substrate Binding to Fe_4S_4 Clusters through Remote Steric Effects. *Inorg. Chem.* **2019**, *58* (8), 5273−5280.
(20) Cecconi, F.; Ghilardi, C. A.; Midollini, S.; Orlandini, A.; Zanello, P. Synthesis, Properties and Structures of the Two "Electron Rich" Cobalt-Sulphur Clusters $[Co_6(\mu_3\text{-}S)_8(PEt_3)_6]^{1+,0}$. *Polyhedron* **1986**, *5* (12), 2021−2031.
(21) Diana, E.; Gervasio, G.; Rossetti, R.; Valdemarin, F.; Bor, G.; Stanghellini, P. L. $Co_6(\mu_3\text{-}S)_8(CO)_6\bullet 3S_8$. Structure, Bonding, and Vibrational Analysis of an Exceptionally Electron-Rich Carbonyl Cluster. *Inorg. Chem.* **1991**, *30* (2), 294−299.
(22) Steigerwald, M. L.; Siegrist, T.; Stuczynski, S. M. $(Et_3P)_6Co_6Te_8$ and a Connection between Chevrel Clusters and the NiAs Structure. *Inorg. Chem.* **1991**, *30* (10), 2256−2257.
(23) Goddard, C. A.; Long, J. R.; Holm, R. H. Synthesis and Characterization of Four Consecutive Members of the Five-Member $[Fe_6S_8(PEt_3)_6]^{N+}$ (n = 0−4) Cluster Electron Transfer Series. *Inorg. Chem.* **1996**, *35* (15), 4347−4354.
(24) Saito, T.; Yamamoto, N.; Yamagata, T.; Imoto, H. Synthesis of $[Mo_6S_8(PEt_3)_6]$ by Reductive Dimerization of a Trinuclear Molybdenum Chloro Sulfido Cluster Complex Coordinated with Triethylphosphine and Methanol: A Molecular Model for Superconducting Chevrel Phases. *J. Am. Chem. Soc.* **1988**, *110* (5), 1646−1647.
(25) Champsaur, A. M.; Velian, A.; Paley, D. W.; Choi, B.; Roy, X.; Steigerwald, M. L.; Nuckolls, C. Building Diatomic and Triatomic Superatom Molecules. *Nano Lett.* **2016**, *16* (8), 5273−5277.
(26) Champsaur, A. M.; Hochuli, T. J.; Paley, D. W.; Nuckolls, C.; Steigerwald, M. L. Superatom Fusion and the Nature of Quantum Confinement. *Nano Lett.* **2018**, *18* (7), 4564−4569.
(27) Kephart, J. A.; Mitchell, B. S.; Chirila, A.; Anderton, K. J.; Rogers, D.; Kaminsky, W.; Velian, A. Atomically Defined Nanopropeller $Fe_3Co_6Se_8(Ph_2PNTol)_6$: Functional Model for the Electronic Metal-Support Interaction Effect and High Catalytic Activity for Carbodiimide Formation. *J. Am. Chem. Soc.* **2019**, *141* (50), 19605−19610.
(28) Mitchell, B. S.; Kaminsky, W.; Velian, A. Tuning the Electronic Structure of Atomically Precise Sn/Co/Se Nanoclusters via Redox Matching of Tin(IV) Surface Sites. *Inorg. Chem.* **2021**, *60* (9), 6135−6139.
(29) Fenske, D.; Ohmer, J.; Hachgenei, J. New Co and Ni Clusters with Se and PPh_3 as Ligands: $Co_4(\mu_3\text{-}Se)_4(PPh_3)_4$, $Co_6(\mu_3\text{-}Se)_8(PPh_3)_6$, $Co_9(\mu_4\text{-}Se)_3(\mu_3\text{-}Se)_8(PPh_3)_6$, and $Ni_{34}(\mu_5\text{-}Se)_2(\mu_4\text{-}Se)_{20}(PPh_3)_{10}$. *Angew. Chem., Int. Ed. Engl.* **1985**, *24* (11), 993−995.
(30) Roy, X.; Schenck, C. L.; Ahn, S.; Lalancette, R. A.; Venkataraman, L.; Nuckolls, C.; Steigerwald, M. L. Quantum Soldering of Individual Quantum Dots. *Angew. Chem., Int. Ed.* **2012**, *51* (50), 12473−12476.
(31) Hernández Sánchez, R.; Champsaur, A. M.; Choi, B.; Wang, S. G.; Bu, W.; Roy, X.; Chen, Y. S.; Steigerwald, M. L.; Nuckolls, C.; Paley, D. W. Electron Cartography in Clusters. *Angew. Chem., Int. Ed.* **2018**, *57* (42), 13815−13820.
(32) Kanatzidis, M. G.; Hagen, W. R.; Dunham, W. R.; Lester, R. K.; Coucouvanis, D. Metastable Fe/S Clusters. The Synthesis, Electronic Structure, and Transformations of the $[Fe_6S_6(L)_6]^{3-}$ Clusters (L = Cl^-, Br^-, I^-, RS^-, RO^-) and the Structure of $[(C_2H_5)_4N]_3[Fe_6S_6Cl_6]$. *J. Am. Chem. Soc.* **1985**, *107* (4), 953−961.
(33) Choi, B.; Paley, D. W.; Siegrist, T.; Steigerwald, M. L.; Roy, X. Ligand Control of Manganese Telluride Molecular Cluster Core Nuclearity. *Inorg. Chem.* **2015**, *54* (17), 8348−8355.
(34) Steigerwald, M. L. Clusters as Small Solids. *Polyhedron* **1994**, *13* (8), 1245−1252.
(35) Stuczynski, S. M.; Kwon, Y. U.; Steigerwald, M. L. The Use of Phosphine Chalcogenides in the Preparation of Cobalt Chalcogenides. *J. Organomet. Chem.* **1993**, *449* (1−2), 167−172.
(36) Ulantikov, A. A.; Gayfulin, Y. M.; Ivanov, A. A.; Sukhikh, T. S.; Ryzhikov, M. R.; Brylev, K. A.; Smolentsev, A. I.; Shestopalov, M. A.; Mironov, Y. V. Soluble Molecular Rhenium Cluster Complexes Exhibiting Multistage Terminal Ligands Reduction. *Inorg. Chem.* **2020**, *59* (9), 6460−6470.
(37) Kang, S.; Zheng, H.; Liu, T.; Hamachi, K.; Kanegawa, S.; Sugimoto, K.; Shiota, Y.; Hayami, S.; Mito, M.; Nakamura, T.; Nakano, M.; Baker, M. L.; Nojiri, H.; Yoshizawa, K.; Duan, C.; Sato, O. A Ferromagnetically Coupled Fe_{42} Cyanide-Bridged Nanocage. *Nat. Commun.* **2015**, *6*, 5955.
(38) Lescouëzec, R.; Vaissermann, J.; Ruiz-Pérez, C.; Lloret, F.; Carrasco, R.; Julve, M.; Verdaguer, M.; Dromzee, Y.; Gatteschi, D.; Wernsdorfer, W. Cyanide-Bridged Iron(III)-Cobalt(II) Double Zigzag Ferromagnetic Chains: Two New Molecular Magnetic Nanowires. *Angew. Chem., Int. Ed.* **2003**, *42* (13), 1483−1486.
(39) Tulsky, E. G.; Crawford, N. R. M.; Baudron, A.; Batail, P.; Long, J. R. Cluster-to-Metal Magnetic Coupling: Synthesis and Characterization of 25-Electron $[Re_{6-n}Os_nSe_8(CN)_6]^{(5-n)-}$ (n = 1, 2) Clusters and $\{Re_{6-n}Os_nSe_8[CNCu(Me_6tren)]_6\}^{9+}$ (n = 0, 1, 2) Assemblies. *J. Am. Chem. Soc.* **2003**, *125* (50), 15543−15553.
(40) Zheng, Z.; Holm, R. H. Cluster Condensation by Thermolysis: Synthesis of a Rhomb-Linked $Re_{12}Se_{16}$ Dicluster and Factors Relevant to the Formation of the $Re_{24}Se_{32}$ Tetracluster. *Inorg. Chem.* **1997**, *36* (23), 5173−5178.
(41) Zheng, Z.; Long, J. R.; Holm, R. H. A Basis Set of Re_6Se_8 Cluster Building Blocks and Demonstration of Their Linking Capability: Directed Synthesis of an $Re_{12}Se_{16}$ Dicluster. *J. Am. Chem. Soc.* **1997**, *119* (9), 2163−2171.
(42) Amari, S.; Imoto, H.; Saito, T. Synthesis and Structures of $[Mo_{12}E_{16}(PEt_3)_{10}]$ (E = S, Se). *J. Chin. Chem. Soc.* **1998**, *45* (4), 445−450.
(43) Demir, S.; Jeon, I. R.; Long, J. R.; Harris, T. D. Radical Ligand-Containing Single-Molecule Magnets. *Coord. Chem. Rev.* **2015**, *289*−*290* (1), 149−176.
(44) Thompson, D. W.; Ito, A.; Meyer, T. J. $[Ru(Bpy)_3]^{2+*}$ and Other Remarkable Metal-to-Ligand Charge Transfer (MLCT) Excited States. *Pure Appl. Chem.* **2013**, *85* (7), 1257−1305.
(45) Bista, D.; Sengupta, T.; Reber, A. C.; Khanna, S. N. A Magnetic Superatomic Dimer with an Intense Internal Electric Dipole Moment. *J. Phys. Chem. A* **2021**, *125* (3), 816−824.
(46) Reber, A. C.; Chauhan, V.; Bista, D.; Khanna, S. N. Superatomic Molecules with Internal Electric Fields for Light Harvesting. *Nanoscale* **2020**, *12* (7), 4736−4742.
(47) Yang, J.; Wang, F.; Russell, J. C.; Hochuli, T. J.; Roy, X.; Steigerwald, M. L.; Zhu, X.; Paley, D. W.; Nuckolls, C. Shape Matching in Superatom Chemistry and Assembly. *J. Am. Chem. Soc.* **2020**, *142* (28), 11993−11998.

https://doi.org/10.1021/jacs.1c09901
J. Am. Chem. Soc. 2022, 144, 306−313